JACS
JOURNAL OF THE AMERICAN CHEMICAL SOCIETY
pubs.acs.org/JACS
Article

Pd/SadPhos Enabled Modular and Enantioselective Assembly of Triarylmethanes

Shuai Zhu,[○] Bo Xiao,[○] Meihua Huang,[○] Yi Wu, Tian-Yu Sun,* Junfeng Yang,* Yun-Dong Wu,* and Junliang Zhang*

Cite This: J. Am. Chem. Soc. 2025, 147, 45210−45220
Read Online
ACCESS | Metrics & More | Article Recommendations | Supporting Information

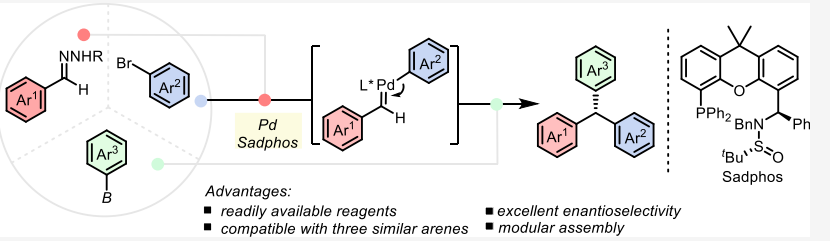

ABSTRACT: Triarylmethanes are important structural motifs with wide applications in natural products, drug discovery, and materials science. Chiral triarylmethanes are particularly noteworthy due to their unique three-dimensional architectures, which facilitate interactions with biological targets. Current enantioselective syntheses primarily rely on strategies such as enantioselective desymmetrization, asymmetric dehydroxylation, and stereocontrolled C−C bond formation. However, these methods often depend on preconstructed frameworks, posing challenges for synthesizing unfunctionalized triarylmethanes. Herein, we present a one-pot cascade reaction that enables the modular and enantioselective synthesis of triarylmethanes from aldehyde-derived hydrazones, aryl halides, and aryl nucleophiles. This method achieves excellent step and pot economies by simultaneously forming two distinct C−C bonds. Notably, the enantiodetermining step is strategically relocated to the transition metal-carbene migratory insertion event, overcoming limitations of conventional approaches. Our results demonstrate robust yields and excellent enantioselectivity across a diverse range of substrates. This modular strategy also allows for facile access to both enantiomers by simply switching the aromatic rings. DFT calculations reveal that the transmetalation step is the rate-determining step and the carbenation process is the enantioselectivity-determining step, also demonstrating the self-adaptive nature of the SadPhos ligand.

INTRODUCTION

Triarylmethanes and their derivatives are classical structural motifs with broad applications in natural products,[1] drug discovery,[2] and materials science (Scheme 1a).[3] Among them, chiral triarylmethanes have garnered significant attention due to their unique three-dimensional architectures, which enable interactions with biological targets and influence material properties.[4] For example, enantioenriched securidanes B has shown good inhibition against PTP1B.[5]

Current enantioselective syntheses of chiral triarylmethane scaffolds mainly employ three primary strategies: (I) enantioselective desymmetrization of preassembled triarylmethane precursors via differentiation of symmetric aryl groups (Scheme 1b);[6] (II) asymmetric dehydroxylation of triarylmethanol to install central chirality (Scheme 1c);[7] and (III) stereocontrolled C−C bond formation between diarylmethyl synthons and aryl partners (Scheme 1d).[8] While desymmetrization and dehydroxylation rely on preconstructed frameworks with an anchoring group as in examples by Yu[6a] and Li,[6c] the latter strategy directly assembles the triarylmethane core through methods such as stereospecific cross-coupling,[8abcde−f] asymmetric Friedel−Crafts arylation,[9] enantioselective conjugate additions,[8e,10] or transition metal-catalyzed C(sp^3)−H activation.[10b,11] The stereospecific cross-coupling reaction establishes chirality through direct transfer from preconfigured chiral diarylmethyl reagents, as has been demonstrated, for instance, by Jarvo,[8a,b] Watson,[8c] and Crudden,[8d] while other catalyst-controlled strategies (e.g., Friedel−Crafts, conjugate additions) are only applicable to electronically activated aromatic systems (such as electron-rich arenes or heteroarenes). Overall, it reveals a universal constraint across contemporary catalytic approaches to triarylmethane synthesis: their mechanistic reliance on the effective differentiation between the steric or electronic biased aromatic ring to achieve high enantioselectivity.[12] This mechanistic requirement, however, poses significant challenges for

Received: August 26, 2025
Revised: November 10, 2025
Accepted: November 12, 2025
Published: November 26, 2025

https://doi.org/10.1021/jacs.5c14810
J. Am. Chem. Soc. 2025, 147, 45210−45220

Scheme 1. Strategies to Access Chiral General Triarylmethanes

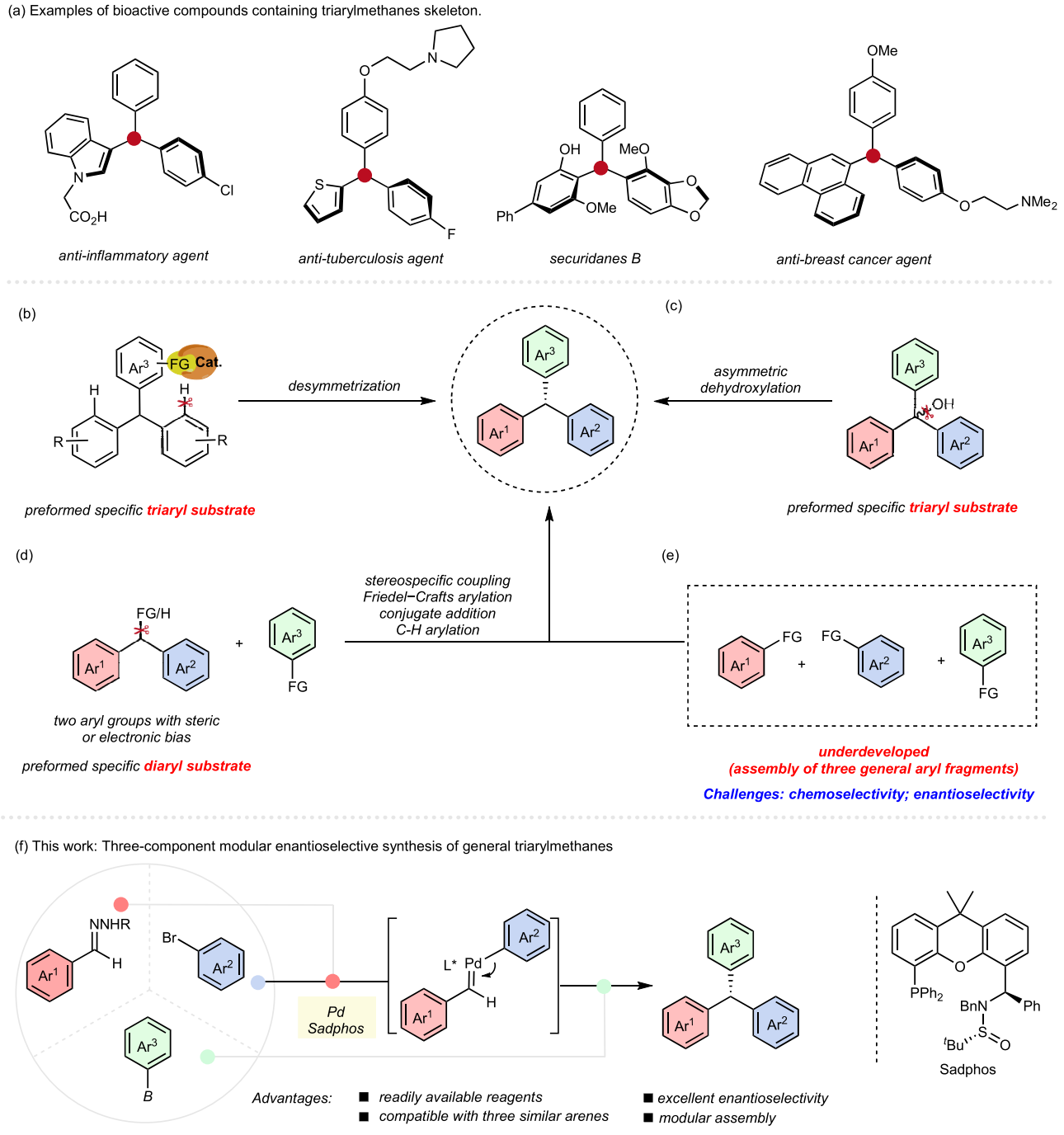

synthesizing triarylmethanes bearing *para*-substituents or unsubstituted heteroarenes as discriminating between electronically or sterically similar rings through weak noncovalent interactions necessitates highly tailored ligands. Consequently, the development of general catalytic methods for enantioselective triarylmethane synthesis—particularly those that forego directing groups—is still highly desirable.

Recently, the modular enantioselective assembly strategy has emerged as a compelling strategy by enabling green, atom-economical access to stereochemically complex architectures.[13] Building on this foundation, our approach advances this paradigm through a novel one-pot cascade coupling of aldehyde-derived hydrazones, aryl halides, and aryl nucleophiles, which simultaneously forge two distinct C−C bonds with excellent step- and pot-economy (Scheme 1e). Most importantly, a critical distinction of this coupling strategy resides in the strategic relocation of the enantiodetermining step to the transition metal-carbene migratory insertion event, a fundamentally distinct stereochemical pathway contrasted with conventional aryl group differentiation approaches, which face inherent geometric limitations in distinguishing isosteric aromatic substrates. Nevertheless, it is worth noting that this approach introduces three critical challenges: (1) achieving precise efficient transition-metal carbene migratory insertion to ensure both efficiency and enantioselectivity;[14] (2) suppressing competing two-component coupling pathways (hydrazone-aryl halide or hydrazone-nucleophile),[15] and (3) prohibiting the facile racemization of the triarylmethane product. Encouraged

https://doi.org/10.1021/jacs.5c14810
J. Am. Chem. Soc. 2025, 147, 45210−45220

Table 1. Optimization of Reaction Conditions[a]

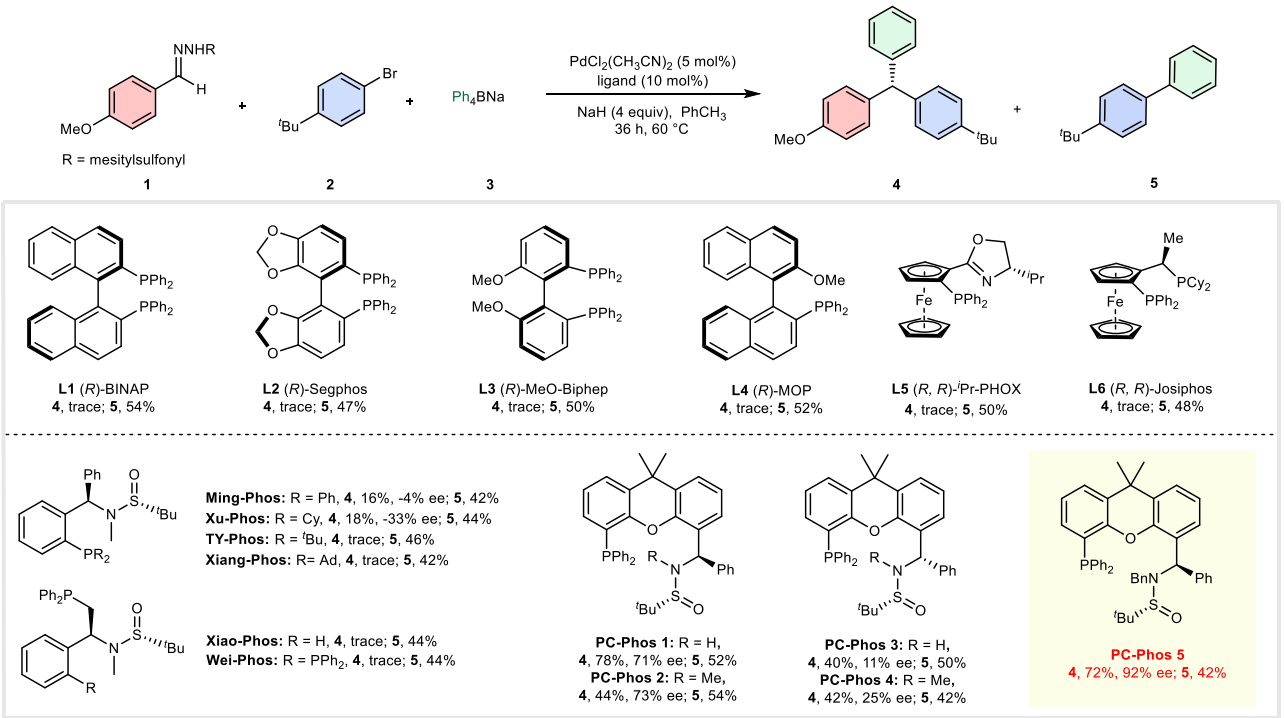

entry	variation of standard conditions	yield of **4** (%)[b]	ee (%)[c]	yield of **5** (%)[d]
1	none	72	92	48
2	THF instead of toluene	10	47	-
3	CH_3CN instead of toluene	-	-	-
4	*n*-hexane instead of toluene	8	49	5
5	NaO^{t}Bu instead of NaH	24	42	19
6	LiO^{t}Bu instead of NaH	42	88	68
7	NaOH instead of NaH	72	88	68
8	$Pd(dba)_2$ instead of $Pd(CH_3CN)_2Cl_2$	74	86	50
9	$Pd(OAc)_2$ instead of $Pd(CH_3CN)_2Cl_2$	44	85	50
10	$Pd(TFA)_2$ instead of $Pd(CH_3CN)_2Cl_2$	68	88	54
11	$PhB(OH)_2$ instead of $NaBPh_4$	10	4	35
12	$PhBPin_3$ instead of $NaBPh_4$	20	24	trace
13	$(PhOB)_3$ instead of $NaBPh_4$	38	25	22

[a]Reaction conditions: **1** (0.1 mmol), **2** (0.3 mmol), **3** (0.2 mmol), $Pd(CH_3CN)_2Cl_2$ (5 mol %), **L** (10 mol %), and NaH (4 equiv) in toluene (0.05 M) at 60 °C under N_2. [b]^{1}H NMR yield with CH_2Br_2 as an internal standard. [c]ee value was determined by chiral HPLC analysis. [d]GC yield with tetradecane as an internal standard.

by our previous work and the wide application of sulfinamide phosphine ligands (SadPhos) in asymmetric multicomponent coupling reactions[16] and cascade reactions,[17] as well as its self-adaptive ability to enable distinct coordination patterns in different elementary steps, we report herein a highly modular and stereoselective route toward triarylmethanes from hydrazones, aryl halides, and aryl borate by palladium catalysis and SadPhos (Scheme 1f).

RESULTS AND DISCUSSION

Exploration of Reaction Conditions. Initially, *N*-mesitylsulfonylhydrazone **1**, 4-*tert*-butylphenyl bromide **2**, and sodium tetraphenylboron **3**, were selected as model substrates to explore the reaction conditions (Table 1). Our initial investigations focused on screening a series of commercially available bisphosphine and monophosphine ligands. However, these efforts did not yield the desired product, with the coupling of aryl bromide (**2**) and borate (**3**) being the sole detected outcome. Further exploration of SadPhos ligands proved to be more promising. Notably, the use of **PC-Phos 2** delivered the desired product in 44% yield with 73% enantiomeric excess (ee). Other SadPhos ligands featuring different skeletons exhibited an inferior performance. Subsequent fine-tuning of the *N*-substituents revealed that **PC-Phos 5** provided the best results, affording the product in 72% yield with 92% ee. A series of optimization experiments demonstrated that the combination of NaH as the base, toluene as the solvent, and tetraarylborate as the nucleophile delivered the highest yield and enantioselectivity. Interestingly, variations in the palladium precatalyst had a minimal impact on reactivity and selectivity (entries 8−10). Furthermore, the choice of a diazo surrogate had a significant impact on the efficiency of the reaction. When *N*-trisylhydrazone or *N*-tosylhydrazone was used as the hydrazine precursor, lower yields were obtained (see Supporting Information for details).[18] This observation indicates that the rate of carbene

https://doi.org/10.1021/jacs.5c14810
J. Am. Chem. Soc. 2025, 147, 45210−45220

Scheme 2. Substrate Scope of Aryl Halides[a]

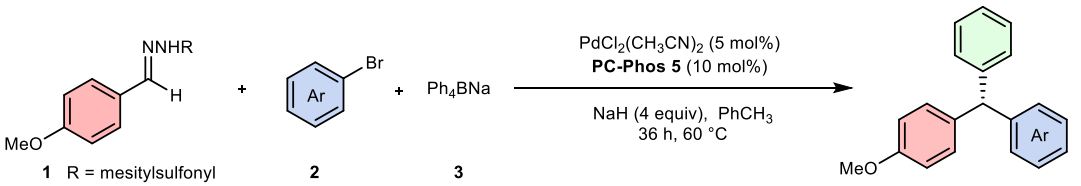

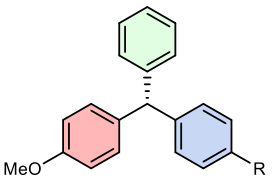

4, R = ^{t}Bu, 64%, 92% ee
6, R = Me, 63%, 90% ee
7, R = Et, 61%, 91% ee
8, R = ^{i}Bu, 69%, 93% ee
9, R = ^{i}Pr, 64%, 90% ee
10, R = ^{n}Pr, 71%, 92% ee
11, R = ^{n}Bu,70%, 92% ee
12, R = OEt, 53%, 90% ee
13, R = OMOM, 41%, 88% ee
14, R = OCF_3, 61%, 90% ee
15, R = TMS, 42%, 91% ee
16, R = F, 68%, 92% ee
17, R = Cl, 40%, 91% ee
18, R = CF_3, 66%, 90% ee
19, R = CO_2Me, 68%, 92% ee
20, R = COMe, 61%, 88% ee
21, R = COPh, 56%, 86% ee

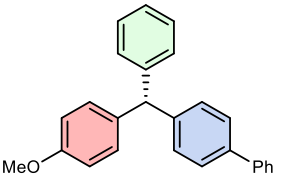

22, 67%, 92% ee

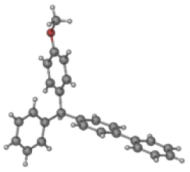

22, CCDC: 2343056

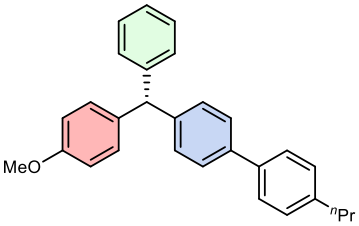

23, 66%, 91% ee

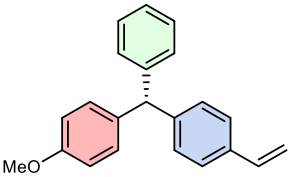

24, 52%, 90% ee

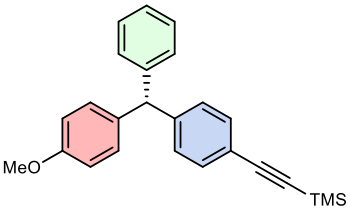

25, 66%, 91% ee

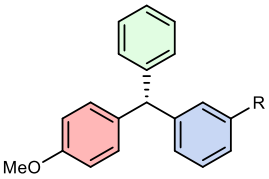

26, R = OMe, 52%,92% ee
27, R = Ph, 64%, 95% ee
28, R = ^{t}Bu, 63%, 92% ee

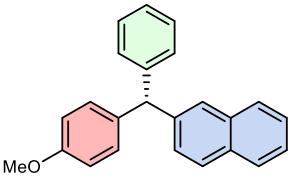

29, 65%, 92% ee

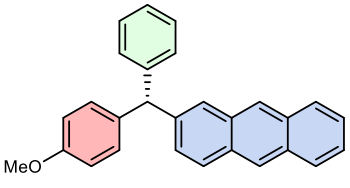

30, 61%, 94% ee

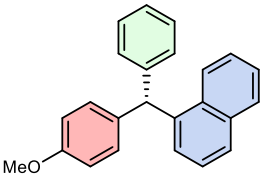

31, 40%, 83% ee

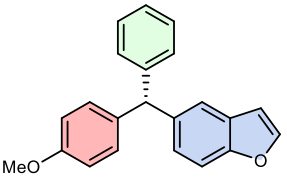

32,51%, 90% ee

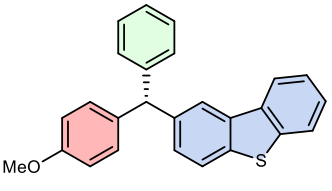

33, 64%, 94% ee

[a]Reaction conditions: **1** (0.3 mmol), **2** (0.9 mmol), **3** (0.6 mmol), $Pd(CH_3CN)_2Cl_2$ (5 mol %), **PC-Phos 5** (10 mol %), and NaH (4 equiv) in $PhCH_3$ (0.05 M) at 60 °C under N_2. Isolated yields; ee value was determined by chiral HPLC analysis.

formation did not correlate with product formation. More notably, the nucleophilic boron species had a profound impact on both the yield and selectivity. Sodium tetraarylborate exhibited highest yields compared with other boron species, probably due to its exquisite reactivity in transferring its aryl group to palladium without the aid of an additional base (entries 11−13).[19] This result also indicates that transmetalation is likely the rate-determining step (vide infra).

Substrate Generality. A wide range of aryl bromides containing various electron-donating (**4**−**15**) and electron-withdrawing (**16**−**21**) groups at the *para*-position were well-tolerated in this reaction (Scheme 2). For instance, functional groups such as alkyl (**4**−**11**), ether (**12**−**14**), silyl (**15**), fluoro (**16**), chloro (**17**), trifluoromethyl (**18**), ester (**19**), and ketone (**20**−**21**) were all compatible, yielding the desired products in moderate-to-good yields and enantioselectivities. The absolute configuration of product **22** was determined to be R by X-ray crystallography. Notably, aryl halides bearing strong electron-withdrawing substituents (**18**−**21**) also performed well, despite the potential for racemization due to the presence of acidic protons. This robustness underscores the versatility of the protocol. Additionally, functional groups such as alkenes (**24**) and alkynes (**25**) were also tolerated, achieving good enantioselectivity (52−66% yield, 90−91% ee). One significant advantage of this protocol is its ability to efficiently access enantioenriched triarylmethanes bearing structurally identical substituents, such as methoxy and ethoxy groups at the *para*-position of the phenyl ring (**12**). Likewise, substituents at the meta-position exhibited minimal impact on reaction efficiency (**26**−**30**). However, ortho-substituted aryl bromides exhibited slightly lower yields and enantioselectivities, likely due to steric hindrance (**31**). Furthermore, heteroaryl bromides, including

https://doi.org/10.1021/jacs.5c14810
J. Am. Chem. Soc. 2025, 147, 45210−45220

Scheme 3. Scope of Different Hydrazones and Aryl Boron Reagents[a]

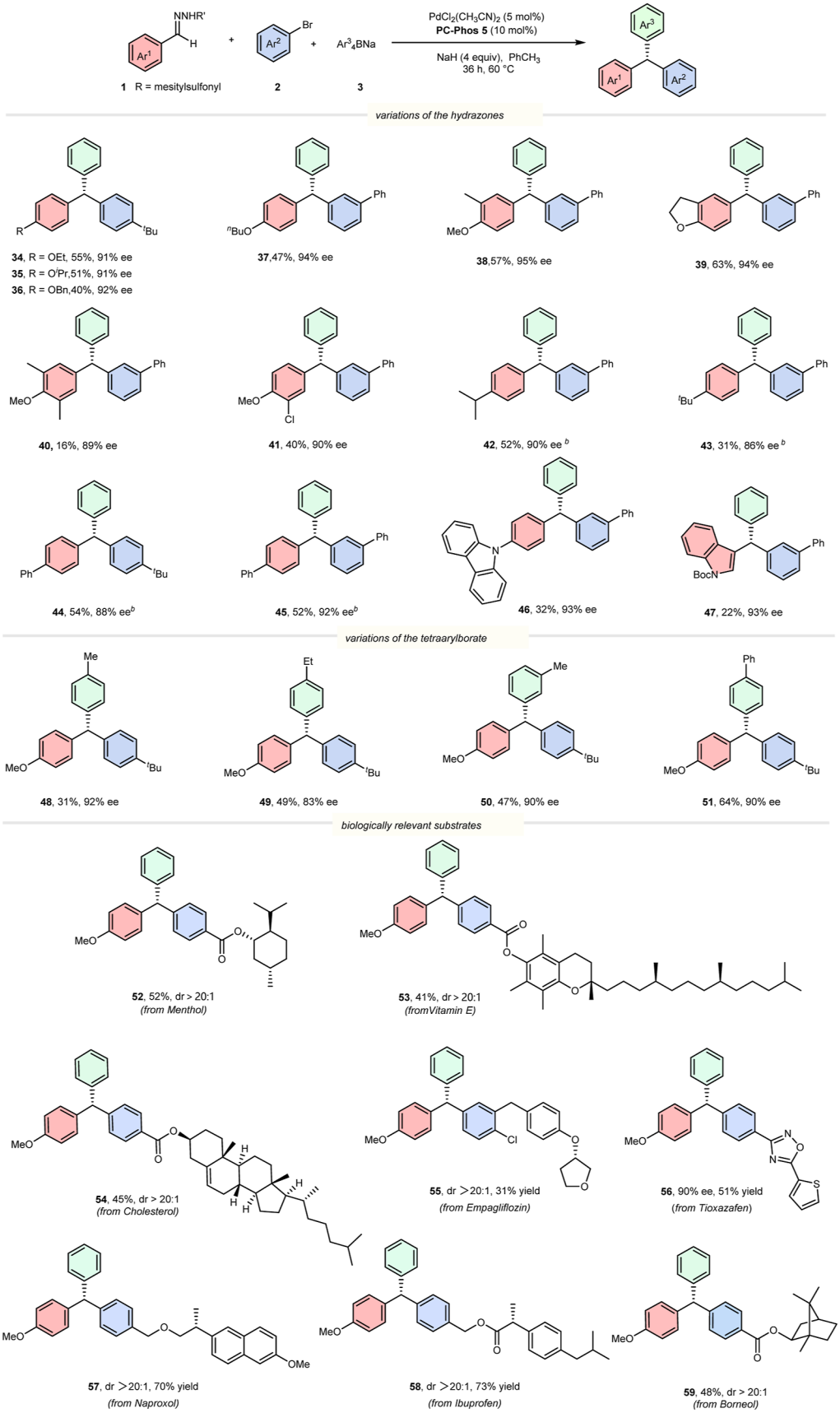

[a]Reaction conditions: **1** (0.3 mmol), **2** (0.9 mmol), **3** (0.6 mmol), $Pd(CH_3CN)_2Cl_2$ (5 mol %), **PC-Phos 5** (10 mol %), and NaH (4 equiv) in $PhCH_3$ (0.05 M) at 60 °C under N_2. Isolated yields; ee value was determined by chiral HPLC analysis. [b]R′ = 1-Naphthalenesulfonyl.

https://doi.org/10.1021/jacs.5c14810
J. Am. Chem. Soc. 2025, 147, 45210−45220

Scheme 4. Facile Preparation of Enantiomers[a]

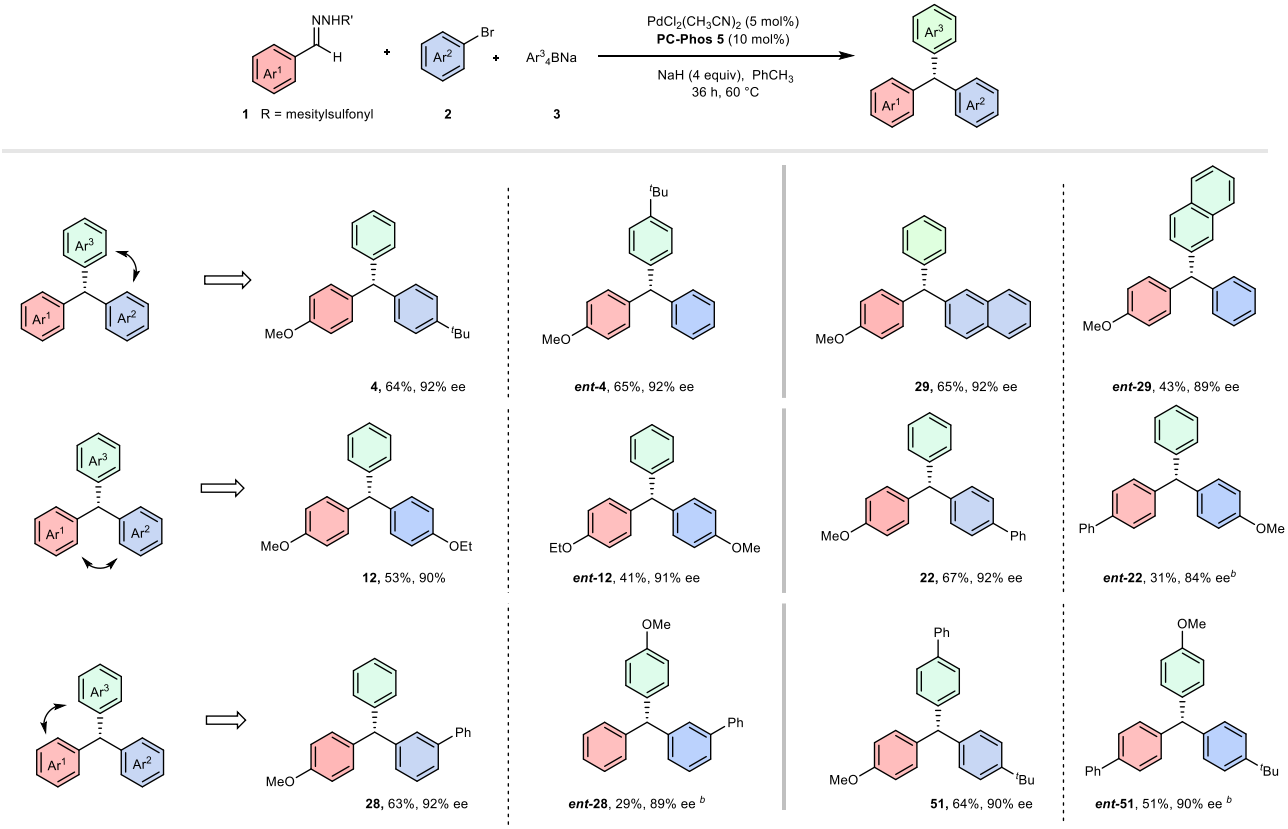

[a]Reaction conditions: **1** (0.3 mmol), **2** (0.9 mmol), **3** (0.6 mmol), $Pd(CH_3CN)_2Cl_2$ (5 mol %), **PC-Phos 5** (10 mol %), and NaH (4 equiv) in $PhCH_3$ (0.05 M) at 60 °C under N_2. Isolated yields; ee value was determined by chiral HPLC analysis. [b]R′ = 1-Naphthalenesulfonyl.

benzofuran (**32**) and dibenzothiophene (**33**), were also successfully employed in this system, delivering products in moderate-to-good yields with high enantioselectivities (51−64% yield, 90−94% ee).

The scope of arylhydrazones was systematically investigated (Scheme 3), revealing excellent functional group tolerance for both *para*- and *meta*-substituents on *N*-mesitylsulfonylhydrazones (**34**−**45**). These substrates smoothly afforded the desired chiral triarylmethanes in good yields. Notably, the electronic nature of the *para*-substituents significantly influenced the reaction outcomes. Specifically, when arylhydrazones bearing strong electron-withdrawing groups were employed, the target compounds were nearly undetectable. However, this limitation could be circumvented by simply exchanging the aromatic moieties between the arylhydrazones and aryl bromides (vide infra). High enantioselectivities were achieved for arylhydrazones bearing heteroaromatic motifs, such as indole and carbazole (**46**−**47**), although the corresponding yields were relatively lower. Additionally, variations in the borate reagents were explored. Borates bearing representative functional groups, such as alkyl and methoxy substituents, delivered the corresponding products (**48**−**51**) in moderate yields but with excellent stereoselectivities (31−64% yield, 83−92% ee). Furthermore, a variety of aryl halides containing bioactive motifs—such as menthol, vitamin E, borneol, cholesterol, and so on—were successfully incorporated into the coupling reaction (**52**−**59**). These substrates delivered chiral triarylmethanes with good yields and diastereoselectivities, demonstrating the broad compatibility of this protocol.

A significant advantage of this modular strategy is the facile access to both enantiomers by simply switching the aromatic rings in the hydrazones, aryl bromides, and aryl boron reagents (Scheme 4). This approach enabled the synthesis of six enantiomers with good to excellent enantioselectivities (84−92% ee), highlighting the flexibility and practicality of the method. However, it is notable that this strategy is not applicable to aryl bromides bearing electron-withdrawing groups.

Synthetic Applications. To further demonstrate the utility of this modular strategy, we conducted a gram-scale reaction using product **19** under standard conditions, achieving a 52% yield and 92% ee (Scheme 5a). The retained ester groups in **19** can be readily converted into alcohols and other esters through reduction, nucleophilic addition, and transesterification reactions (Scheme 5b). Importantly, the presence of strong bases during these transformations did not compromise the enantioselectivity. Moreover, this protocol can be applied to the synthesis of bioactive compounds. For instance, an antitubercular agent (**63**)[2d] that has not been previously reported in the context of asymmetric catalysis can be efficiently synthesized using this method (Scheme 5c).

Mechanistic Studies. To elucidate the reaction mechanism, density functional theory (DFT) calculations were performed at the M06-L/SDD/6-311++G(d,p)/SMD//B3LYP-D3/LANL2DZ/6-31G(d,p) level of theory. The Pd(0) species **INT1** was selected as the reference point for the catalytic cycle (Scheme 6a). In **INT1**, the distance between the benzylic hydrogen atom in **PC-Phos 5** and the Pd center is 2.25 Å, indicating the presence of a Pd···H anagostic

https://doi.org/10.1021/jacs.5c14810
J. Am. Chem. Soc. 2025, 147, 45210−45220

Scheme 5. Gram-Scale Reaction and Product Elaboration[a]

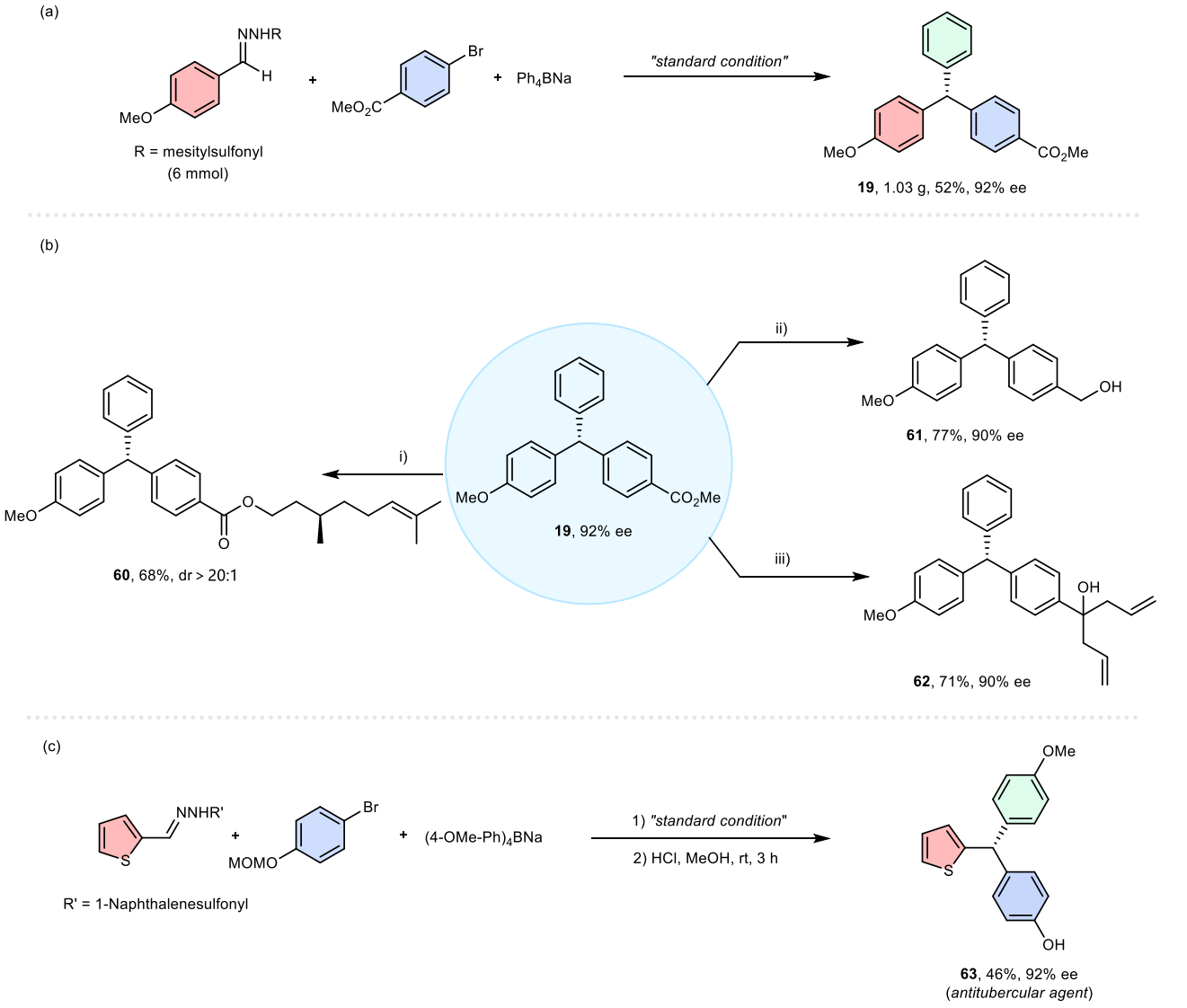

[a]Reaction conditions: (i) L-citronellol (3 equiv), LiHMDS (2 equiv) rt, 3 h, and neat; (ii) $LiAlH_4$ (2 equiv), THF, and rt; and (iii) AllylMgBr (2.0 equiv), THF, and rt.

interaction.[20] The Pd···H anagostic interaction is observed in most intermediates and transition states on the potential energy surface (PES), where it contributes to their stabilization. Our previous work[16] demonstrated that Pd(0) species preferentially undergo oxidative addition with Ar^2Br rather than carbenation with Ar^1CHN_2. Accordingly, **INT1** proceeds through oxidative addition via −P,O coordinated **TS1** to afford the Pd(II) intermediate **INT2**, with an activation barrier of 12.7 kcal/mol. Two possible reaction pathways were subsequently investigated for **INT2**: (1) transmetalation leading to a two-component coupling byproduct (red line) and (2) carbenation resulting in a three-component coupling product (black line). In the transmetalation pathway, **INT2** reacts with borate via **TS5** to generate intermediate **INT5**, with an activation barrier of 13.9 kcal/mol. **INT5** then undergoes facile reductive elimination via **TS6** to yield the two-component byproduct Ar^2Ph. Alternatively, carbenation of **INT2** with Ar^1CHN_2 proceeds through **TS2** with an activation barrier of 12.5 kcal/mol, which is 1.4 kcal/mol lower in energy than that of **TS5**. Intrinsic reaction coordinate (IRC) calculations on **TS2** led to the exothermic formation of **INT3**, in which the carbene has been inserted into the Pd−Ar^2 bond. **INT3** then undergoes transmetalation via **TS3** to form **INT4** ($\Delta G^{\ddagger}$ = 26.1 kcal/mol), followed by reductive elimination (**TS4**, $\Delta G^{\ddagger}$ = 23.3 kcal/mol) to deliver the target three-component coupling product **PRO**, completing the catalytic cycle with regeneration of the Pd(0) species.

Since the reactions become irreversible after passing through **TS2** and **TS5**, the energy barrier difference between **TS2** and **TS5** determines the product selectivity. **TS2** has a 1.4 kcal/mol lower activation barrier than **TS5**, indicating that the three-component coupling pathway is the more favorable pathway than the two-component coupling pathway. This computational result is consistent with experimental observations.

Overall, the catalytic cycle is initiated by the oxidative addition of **INT1** to form **INT2**, followed by a stereoselectivity-determining carbenation step that affords **INT3**. Subsequent transmetalation and reductive elimination steps complete the cycle, delivering the desired product. Among these steps, the transmetalation of **INT3** is identified as the

https://doi.org/10.1021/jacs.5c14810
J. Am. Chem. Soc. 2025, 147, 45210−45220

Scheme 6. DFT Calculations

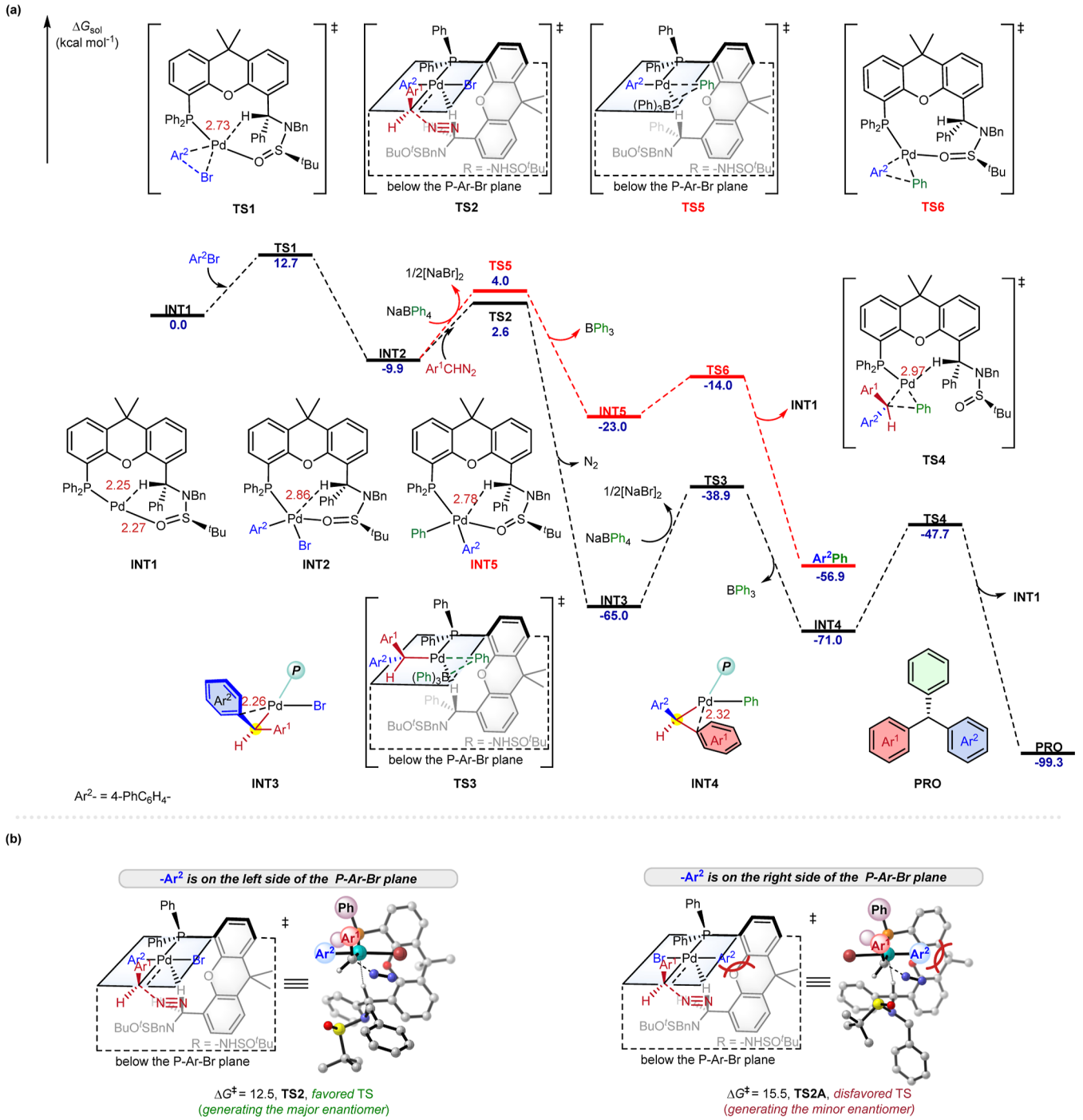

rate-determining step. Notably, the efficiency of the three-component coupling is attributed to the higher activation barrier for the transmetalation of **INT2** compared to carbenation.

Guided by the computed PES, we further investigated the origin of the enantioselectivity during the carbenation step (Scheme 6b). Due to the strong *trans* effect between the phosphorus donor and either the $-Ar^2$ or $-Br$ substituent, configurations in which the phosphorus atom lies *trans* to $-Ar^2$ or $-Br$ are energetically disfavored.[21] Consequently, positioning the carbene precursor *trans* to the phosphorus ligand affords a lower-energy carbenation transition state.[22] Among the carbenation transition states examined (see Figure S3 in Supporting Information), **TS2** and **TS2A** were identified as the most stable transition states leading to the major and minor enantiomers, respectively. In **TS2**, leading to the major enantiomer, the $-Ar^2$ group is oriented away from the ligand, toward the less hindered (left) side. In contrast, in **TS2A**, which gives rise to the minor enantiomer, the $-Ar^2$ group is directed toward the more sterically congested (right) side of the ligand, resulting in significant steric repulsion. The calculated free energy difference between **TS2A** and **TS2** is 3.0 kcal/mol (ΔG(**TS2A**) − ΔG(**TS2**)), consistent with the experimentally observed high enantioselectivity. Notably,

https://doi.org/10.1021/jacs.5c14810
J. Am. Chem. Soc. 2025, 147, 45210−45220

unlike the bidentate −P,O coordinated transition state involved in oxidative addition, **PC-Phos** adopts a monodentate −P coordination mode during carbenation. Additionally, a Pd···H anagostic interaction is formed between the H on the ligand's side arm and the Pd center, which locks the ligand in a specific orientation to modulate the enantioselectivity. Therefore, the side arm of **PC-Phos** not only serves as a flexible auxiliary coordination site but also facilitates noncovalent interactions that enhance stereocontrol. The SadPhos ligand exhibits remarkable structural adaptability, adopting distinct coordination modes across different elementary steps, thereby promoting both catalytic activity and enantioselectivity.[17d,23]

CONCLUSION

In summary, we have developed a modular and enantioselective strategy for the assembly of chiral triarylmethanes. This method features high step and pot economies, along with operational simplicity, enabling the simultaneous formation of two C−C bonds in a cascade and enantioselective fashion. The protocol provides efficient access to both enantiomers of the product using a single catalyst simply by switching the aryl coupling partners. DFT-based mechanistic investigations revealed that the SadPhos ligand exhibits a pronounced structural adaptability and flexible coordination behavior throughout the catalytic cycle. The concerted carbene formation/migratory insertion process was identified as the enantiodetermining step, while transmetalation constitutes the rate-determining step. We anticipate that this asymmetric triarylmethane strategy will not only deepen our understanding of ligand adaptability in transition-metal catalysis but also unlock greater potential for developing challenging multiple carbon−carbon and carbon−heteroatom bond formations, thereby advancing the development of cross-coupling methodologies in organic synthesis.

ASSOCIATED CONTENT

Supporting Information

The Supporting Information is available free of charge at https://pubs.acs.org/doi/10.1021/jacs.5c14810.

Experimental procedures, compound characterization data, copies of NMR spectra, and chiral HPLC chromatograms (PDF)

DFT calculations, resting state of the catalytic cycle, oxidative addition of Pd(0) species, carbenation of Pd(II) species, transmetalation of Pd(II) species, reductive elimination of Pd(II) species INT5, energies for optimized structures, and coordinates (PDF)

Accession Codes

Deposition Number 2343056 contains the supplementary crystallographic data for this paper. These data can be obtained free of charge via the joint Cambridge Crystallographic Data Centre (CCDC) and Fachinformationszentrum Karlsruhe Access Structures service.

AUTHOR INFORMATION

Corresponding Authors

Tian-Yu Sun − *Key Laboratory of Computational Chemistry and Drug Design, State Key Laboratory of Chemical Oncogenomics, Shenzhen Key Laboratory of Chemical Genomics, School of Chemical Biology and Biotechnology, Peking University Shenzhen Graduate School, Shenzhen 518055, China;* orcid.org/0000-0002-7746-479X; Email: tian-yu_sun@pku.edu.cn

Junfeng Yang − *State Key Laboratory of Green Chemical Synthesis and Conversion, Department of Chemistry, Fudan University, Shanghai 200438, China; School of Chemistry and Chemical Engineering, Henan Normal University, Xinxiang, Henan 453007, China; School of Chemistry & Chemical Engineering, Yangzhou University, Yangzhou 225002, China;* orcid.org/0000-0001-5209-1301; Email: yangjf@fudan.edu.cn

Yun-Dong Wu − *Key Laboratory of Computational Chemistry and Drug Design, State Key Laboratory of Chemical Oncogenomics, Shenzhen Key Laboratory of Chemical Genomics, School of Chemical Biology and Biotechnology, Peking University Shenzhen Graduate School, Shenzhen 518055, China; College of Chemistry and Molecular Engineering, Peking University, Beijing 100871, China;* orcid.org/0000-0003-4477-7332; Email: wuyd@pkusz.edu.cn

Junliang Zhang − *State Key Laboratory of Green Chemical Synthesis and Conversion, Department of Chemistry, Fudan University, Shanghai 200438, China; School of Chemistry and Chemical Engineering, Henan Normal University, Xinxiang, Henan 453007, China; School of Chemistry & Chemical Engineering, Yangzhou University, Yangzhou 225002, China; State Key Laboratory of Organometallic Chemistry, Shanghai Institute of Organic Chemistry, Chinese Academy of Sciences, Shanghai 200032, China;* orcid.org/0000-0002-4636-2846; Email: junliangzhang@fudan.edu.cn

Authors

Shuai Zhu − *State Key Laboratory of Green Chemical Synthesis and Conversion, Department of Chemistry, Fudan University, Shanghai 200438, China*

Bo Xiao − *Key Laboratory of Computational Chemistry and Drug Design, State Key Laboratory of Chemical Oncogenomics, Shenzhen Key Laboratory of Chemical Genomics, School of Chemical Biology and Biotechnology, Peking University Shenzhen Graduate School, Shenzhen 518055, China; Hoffmann Institute of Advanced Materials, School of Food and Drug, Shenzhen Polytechnic University, Shenzhen 518055, China*

Meihua Huang − *Changchun University of Technology, Changchun 130012, China*

Yi Wu − *State Key Laboratory of Green Chemical Synthesis and Conversion, Department of Chemistry, Fudan University, Shanghai 200438, China*

Complete contact information is available at: https://pubs.acs.org/10.1021/jacs.5c14810

Author Contributions

○S.Z., B.X., and M.H. contributed equally to this work.

Notes

The authors declare no competing financial interest.

ACKNOWLEDGMENTS

We gratefully acknowledge the funding support of National Key R&D Program of China (No. 2021YFF0701600), NSFC (22271053, 22031004, 21921003, 22403067), STCSM (21ZR1445900), Shanghai Municipal Education Commission (20212308), and Shenzhen Polytechnic University Research

Fund (6025310040K). This work was supported by Shenzhen Bay Laboratory High Performance Computing and Informatics Facility.

REFERENCES

(1) (a) Baba, K.; Maeda, K.; Tabata, Y.; Doi, M.; Kozawa, M. Chemical Studies on the Heartwood of Cassia garrettiana CRAIB. III. Structures of Two New Polyphenolic Compounds. *Chem. Pharm. Bull.* **1988**, *36*, 2977−2983. (b) Snyder, S. A.; Breazzano, S. P.; Ross, A. G.; Lin, Y.; Zografos, A. L. Total Synthesis of Diverse Carbogenic Complexity within the Resveratrol Class from a Common Building Block. *J. Am. Chem. Soc.* **2009**, *131*, 1753−1765.

(2) (a) Kandela, I. K.; Bartlett, J. A.; Indig, G. L. Effect of molecular structure on the selective phototoxicity of triarylmethane dyes towards tumor cells. *Photochem. Photobiol. Sci.* **2002**, *1*, 309−314. (b) Shagufta; Srivastava, A. K.; Sharma, R.; Mishra, R.; Balapure, A. K.; Murthy, P. S. R.; Panda, G. Substituted phenanthrenes with basic amino side chains: A new series of anti-breast cancer agents. *Bioorg. Med. Chem.* **2006**, *14*, 1497−1505. (c) Das, S. K.; Panda, G.; Chaturvedi, V.; Manju, Y. S.; Gaikwad, A. K.; Sinha, S. Design, synthesis and antitubercular activity of diarylmethylnaphthol derivatives. *Bioorg. Med. Chem. Lett.* **2007**, *17*, 5586−5589. (d) Parai, M. K.; Panda, G.; Chaturvedi, V.; Manju, Y. K.; Sinha, S. Thiophene containing triarylmethanes as antitubercular agents. *Bioorg. Med. Chem. Lett.* **2008**, *18*, 289−292.

(3) (a) Gibson, H. W.; Lee, S. H.; Engen, P. T.; Lecavalier, P.; Sze, J.; Shen, Y. X.; Bheda, M. New triarylmethyl derivatives: "blocking groups" for rotaxanes and polyrotaxanes. *J. Org. Chem.* **1993**, *58*, 3748−3756. (b) Shchepinov, M. S.; Korshun, V. A. Recent applications of bifunctional trityl groups. *Chem. Soc. Rev.* **2003**, *32*, 170−180. (c) Xu, Y.-Q.; Lu, J.-M.; Li, N.-J.; Yan, F.; Xia, X.-W.; Xu, Q.-F. Pseudo-living radical polymerization using triarylmethane as the thermal iniferter. *Eur. Polym. J.* **2008**, *44*, 2404−2411. (d) Mondal, S.; Verma, A.; Saha, S. Conformationally Restricted Triarylmethanes: Synthesis, Photophysical Studies, and Applications. *Eur. J. Org Chem.* **2019**, *2019*, 864−894.

(4) Nambo, M.; Crudden, C. M. Recent Advances in the Synthesis of Triarylmethanes by Transition Metal Catalysis. *ACS Catal.* **2015**, *5*, 4734−4742.

(5) Zhou, B.; Liu, D. X.; Yuan, X. J.; Li, J. Y.; Xu, Y. C.; Li, J.; Li, Y.; Yue, J. M. (−)- and (+)-Securidanes A and B, Natural Triarylmethane Enantiomers: Structure and Bioinspired Total Synthesis. *Research* **2018**, *2018*, 2674182.

(6) (a) Shi, B.-F.; Maugel, N.; Zhang, Y.-H.; Yu, J.-Q. PdII-Catalyzed Enantioselective Activation of C(sp2) H and C(sp3) H Bonds Using Monoprotected Amino Acids as Chiral Ligands. *Angew. Chem., Int. Ed.* **2008**, *47*, 4882−4886. (b) Lu, S.; Song, X.; Poh, S. B.; Yang, H.; Wong, M. W.; Zhao, Y. Access to Enantiopure Triarylmethanes and 1,1-Diarylalkanes by NHC-Catalyzed Acylative Desymmetrization. *Chem.—Eur. J.* **2017**, *23*, 2275−2281. (c) Song, P.; Hu, L.; Yu, T.; Jiao, J.; He, Y.; Xu, L.; Li, P. Development of a Tunable Chiral Pyridine Ligand Unit for Enantioselective Iridium-Catalyzed C−H Borylation. *ACS Catal.* **2021**, *11*, 7339−7349.

(7) Yan, Q.; Duan, M.; Chen, C.; Deng, Z.; Wu, M.; Yu, P.; He, M.-L.; Zhu, G.; Houk, K. N.; Sun, J. Organocatalytic discrimination of non-directing aryl and heteroaryl groups: enantioselective synthesis of bioactive indole-containing triarylmethanes. *Chem. Sci.* **2022**, *13*, 5767−5773.

(8) (a) Taylor, B. L. H.; Harris, M. R.; Jarvo, E. R. Synthesis of Enantioenriched Triarylmethanes by Stereospecific Cross-Coupling Reactions. *Angew. Chem., Int. Ed.* **2012**, *51*, 7790−7793. (b) Harris, M. R.; Hanna, L. E.; Greene, M. A.; Moore, C. E.; Jarvo, E. R. Retention or Inversion in Stereospecific Nickel-Catalyzed Cross-Coupling of Benzylic Carbamates with Arylboronic Esters: Control of Absolute Stereochemistry with an Achiral Catalyst. *J. Am. Chem. Soc.* **2013**, *135*, 3303−3306. (c) Zhou, Q.; Srinivas, H. D.; Dasgupta, S.; Watson, M. P. Nickel-Catalyzed Cross-Couplings of Benzylic Pivalates with Arylboroxines: Stereospecific Formation of Diarylalkanes and Triarylmethanes. *J. Am. Chem. Soc.* **2013**, *135*, 3307−3310. (d) Matthew, S. C.; Glasspoole, B. W.; Eisenberger, P.; Crudden, C. M. Synthesis of Enantiomerically Enriched Triarylmethanes by Enantiospecific Suzuki−Miyaura Cross-Coupling Reactions. *J. Am. Chem. Soc.* **2014**, *136*, 5828−5831. (e) Huang, Y.; Hayashi, T. Asymmetric Synthesis of Triarylmethanes by Rhodium-Catalyzed Enantioselective Arylation of Diarylmethylamines with Arylboroxines. *J. Am. Chem. Soc.* **2015**, *137*, 7556−7559. (f) Lou, Y.; Cao, P.; Jia, T.; Zhang, Y.; Wang, M.; Liao, J. Copper-Catalyzed Enantioselective 1,6-Boration of para-Quinone Methides and Efficient Transformation of gem-Diarylmethine Boronates to Triarylmethanes. *Angew. Chem., Int. Ed.* **2015**, *54*, 12134−12138. (g) Lee, M.; Davies, H. M. L. Enantioselective Synthesis of Triarylmethanes via Intermolecular C−H Functionalization of Cyclohexadienes with Diaryldiazomethanes. *Org. Lett.* **2023**, *25*, 4000−4004.

(9) (a) Sun, F.-L.; Zheng, X.-J.; Gu, Q.; He, Q.-L.; You, S.-L. Enantioselective Synthesis of Unsymmetrical Triarylmethanes by Chiral Brønsted Acids. *Eur. J. Org Chem.* **2010**, *2010*, 47−50. (b) Sun, Y.-Z.; Ren, Z.-Y.; Yang, Y.-X.; Liu, Y.; Lin, G.-Q.; He, Z.-T. Asymmetric Substitution by Alkynyl Copper Driven Dearomatization and Rearomatization. *Angew. Chem., Int. Ed.* **2023**, *62*, No. e202314517.

(10) (a) Liao, H.-H.; Chatupheeraphat, A.; Hsiao, C.-C.; Atodiresei, I.; Rueping, M. Asymmetric Brønsted Acid Catalyzed Synthesis of Triarylmethanes—Construction of Communesin and Spiroindoline Scaffolds. *Angew. Chem., Int. Ed.* **2015**, *54*, 15540−15544. (b) Kim, J. H.; Greßies, S.; Boultadakis-Arapinis, M.; Daniliuc, C.; Glorius, F. Rh(I)/NHC*-Catalyzed Site- and Enantioselective Functionalization of C(sp3)−H Bonds Toward Chiral Triarylmethanes. *ACS Catal.* **2016**, *6*, 7652−7656. (c) Wong, Y. F.; Wang, Z.; Sun, J. Chiral phosphoric acid catalyzed asymmetric addition of naphthols to para-quinone methides. *Org. Biomol. Chem.* **2016**, *14*, 5751−5754. (d) Yue, C.; Na, F.; Fang, X.; Cao, Y.; Antilla, J. C. Chiral Phosphoric Acid Catalyzed Asymmetric Synthesis of Hetero-triarylmethanes from Racemic Indolyl Alcohols. *Angew. Chem., Int. Ed.* **2018**, *57*, 11004−11008. (e) Jiang, F.; Chen, K.-W.; Wu, P.; Zhang, Y.-C.; Jiao, Y.; Shi, F. A Strategy for Synthesizing Axially Chiral Naphthyl-Indoles: Catalytic Asymmetric Addition Reactions of Racemic Substrates. *Angew. Chem., Int. Ed.* **2019**, *58*, 15104−15110. (f) Huang, W.-J.; Ma, Y.-Y.; Liu, L.-X.; Wu, B.; Jiang, G.-F.; Zhou, Y.-G. Chiral Phosphoric Acid-Catalyzed C6 Functionalization of 2,3-Disubstituted Indoles for Synthesis of Heterotriarylmethanes. *Org. Lett.* **2021**, *23*, 2393−2398.

(11) Zhang, Z.-Y.; Gou, B.-B.; Wang, Q.; Gu, Q.; You, S.-L. Rh-catalyzed Asymmetric C(sp3)−H Arylation of 8-Benzylquinolines with Arylboronic Acids. *Adv. Synth. Catal.* **2024**, *366*, 774−779.

(12) (a) Jagannathan, J. R.; Fettinger, J. C.; Shaw, J. T.; Franz, A. K. Enantioselective Si-H Insertion Reactions of Diarylcarbenes for the Synthesis of Silicon-Stereogenic Silanes. *J. Am. Chem. Soc.* **2020**, *142*, 11674−11679. (b) Yang, L.-L.; Evans, D.; Xu, B.; Li, W.-T.; Li, M.-L.; Zhu, S.-F.; Houk, K. N.; Zhou, Q.-L. Enantioselective Diarylcarbene Insertion into Si−H Bonds Induced by Electronic Properties of the Carbenes. *J. Am. Chem. Soc.* **2020**, *142*, 12394−12399. (c) Zhou, H.; Zhou, Y.; Bae, H. Y.; Leutzsch, M.; Li, Y.; De, C. K.; Cheng, G.-J.; List, B. Organocatalytic stereoselective cyanosilylation of small ketones. *Nature* **2022**, *605*, 84−89. (d) Wang, M.; Liu, S.; Liu, H.; Wang, Y.; Lan, Y.; Liu, Q. Asymmetric hydrogenation of ketimines with minimally different alkyl groups. *Nature* **2024**, *631*, 556−562. (e) Wu, W.-Q.; Xie, P.-P.; Wang, L.-Y.; Gou, B.-B.; Lin, Y.; Hu, L.-W.; Zheng, C.; You, S.-L.; Shi, H. Chiral Bis(binaphthyl) Cyclopentadienyl Ligands for Rhodium-Catalyzed Desymmetrization of Diarylmethanes via Selective Arene Coordination. *J. Am. Chem. Soc.* **2024**, *146*, 26630−26638.

(13) (a) Murphy, S. K.; Zeng, M.; Herzon, S. B. A modular and enantioselective synthesis of the pleuromutilin antibiotics. *Science* **2017**, *356*, 956−959. (b) Wei, J.; Zhang, J.; Cheng, J. K.; Xiang, S.-H.; Tan, B. Modular enantioselective access to β-amino amides by Brønsted acid-catalysed multicomponent reactions. *Nat. Chem.* **2023**, *15*, 647−657. (c) Liu, T.; Li, T.; Tea, Z. Y.; Wang, C.; Shen, T.; Lei, Z.; Chen, X.; Zhang, W.; Wu, J. Modular assembly of arenes, ethylene

https://doi.org/10.1021/jacs.5c14810
J. Am. Chem. Soc. 2025, 147, 45210−45220

and heteroarenes for the synthesis of 1,2-arylheteroaryl ethanes. *Nat. Chem.* **2024**, *16*, 1705−1714. (d) Lyu, H.; Tugwell, T. H.; Chen, Z.; Kukier, G. A.; Turlik, A.; Wu, Y.; Houk, K. N.; Liu, P.; Dong, G. Modular synthesis of 1,2-azaborines via ring-opening BN-isostere benzannulation. *Nat. Chem.* **2024**, *16*, 269−276. (e) Ren, L.-Q.; Zhan, B.; Zhao, J.; Guo, Y.; Zu, B.; Li, Y.; He, C. Modular enantioselective assembly of multi-substituted boron-stereogenic BODIPYs. *Nat. Chem.* **2025**, *17*, 83−91.

(14) Xia, Y.; Qiu, D.; Wang, J. Transition-Metal-Catalyzed Cross-Couplings through Carbene Migratory Insertion. *Chem. Rev.* **2017**, *117*, 13810−13889.

(15) (a) Xiao, Q.; Zhang, Y.; Wang, J. Diazo Compounds and N-Tosylhydrazones: Novel Cross-Coupling Partners in Transition-Metal-Catalyzed Reactions. *Acc. Chem. Res.* **2013**, *46*, 236−247. (b) Xia, Y.; Wang, J. Transition-Metal-Catalyzed Cross-Coupling with Ketones or Aldehydes via N-Tosylhydrazones. *J. Am. Chem. Soc.* **2020**, *142*, 10592−10605.

(16) (a) Zhao, G.; Wu, Y.; Wu, H.-H.; Yang, J.; Zhang, J. Pd/GF-Phos-Catalyzed Asymmetric Three-Component Coupling Reaction to Access Chiral Diarylmethyl Alkynes. *J. Am. Chem. Soc.* **2021**, *143*, 17983−17988. (b) Yang, B.; Cao, K.; Zhao, G.; Yang, J.; Zhang, J. Pd/Ming-Phos-Catalyzed Asymmetric Three-Component Arylsilylation of N-Sulfonylhydrazones: Enantioselective Synthesis of gem-Diarylmethine Silanes. *J. Am. Chem. Soc.* **2022**, *144*, 15468−15474.

(17) (a) Wang, L.; Zhang, K.; Wang, Y.; Li, W.; Chen, M.; Zhang, J. Enantioselective Synthesis of Isoxazolines Enabled by Palladium-Catalyzed Carboetherification of Alkenyl Oximes. *Angew. Chem., Int. Ed.* **2020**, *59*, 4421−4427. (b) Pan, Z.; Li, W.; Zhu, S.; Liu, F.; Wu, H.-H.; Zhang, J. Palladium/TY-Phos-Catalyzed Asymmetric Intermolecular α-Arylation of Aldehydes with Aryl Bromides. *Angew. Chem., Int. Ed.* **2021**, *60*, 18542−18546. (c) Xu, B.; Ji, D.; Wu, L.; Zhou, L.; Liu, Y.; Zhang, Z.-M.; Zhang, J. Palladium/Xu-Phos-catalyzed enantioselective cascade Heck/remote C(sp2)−H alkylation reaction. *Chem* **2022**, *8*, 836−849. (d) Li, W.; Zhang, J. Sadphos as Adaptive Ligands in Asymmetric Palladium Catalysis. *Acc. Chem. Res.* **2024**, *57*, 489−513.

(18) Sivaguru, P.; Pan, Y.; Wang, N.; Bi, X. Who is Who in the Carbene Chemistry of N-Sulfonyl Hydrazones. *Chin. J. Chem.* **2024**, *42*, 2071−2108.

(19) (a) For selective examples, see: Kurosawa, H.; Ogoshi, S.; Kawasaki, Y.; Murai, S.; Miyoshi, M.; Ikeda, I. Novel dependency of stereochemistry upon metal, ligand, and solvent in oxidative addition of allylic chloride to palladium(0) and platinum(0) complexes. *J. Am. Chem. Soc.* **1990**, *112*, 2813−2814. (b) Miura, T.; Sasaki, T.; Nakazawa, H.; Murakami, M. Ketone Synthesis by Intramolecular Acylation of Organorhodium(I) with Ester. *J. Am. Chem. Soc.* **2005**, *127*, 1390−1391. (c) Shintani, R.; Tsutsumi, Y.; Nagaosa, M.; Nishimura, T.; Hayashi, T. Sodium Tetraarylborates as Effective Nucleophiles in Rhodium/Diene-Catalyzed 1,4-Addition to β,β-Disubstituted α,β-Unsaturated Ketones: Catalytic Asymmetric Construction of Quaternary Carbon Stereocenters. *J. Am. Chem. Soc.* **2009**, *131*, 13588−13589. (d) Vasu, D.; Yorimitsu, H.; Osuka, A. Palladium-Assisted "Aromatic Metamorphosis" of Dibenzothiophenes into Triphenylenes. *Angew. Chem., Int. Ed.* **2015**, *54*, 7162−7166.

(20) (a) Piers, W. E.; Bercaw, J. E. .alpha. Agostic assistance in Ziegler-Natta polymerization of olefins. Deuterium isotopic perturbation of stereochemistry indicating coordination of an.alpha. carbon-hydrogen bond in chain propagation. *J. Am. Chem. Soc.* **1990**, *112*, 9406−9407. (b) Race, J. J.; Burnage, A. L.; Boyd, T. M.; Heyam, A.; Martínez-Martínez, A. J.; Macgregor, S. A.; Weller, A. S. Ortho-aryl substituted DPEphos ligands: rhodium complexes featuring C−H anagostic interactions and B−H agostic bonds. *Chem. Sci.* **2021**, *12*, 8832−8843.

(21) (a) Han, J.; Xiao, B.; Sun, T.-Y.; Wang, M.; Jin, L.; Yu, W.; Wang, Y.; Fang, D.-M.; Zhou, Y.; Wu, X.-F.; Wu, Y.-D.; Liao, J. Enantioselective Double Carbonylation Enabled by High-Valent Palladium Catalysis. *J. Am. Chem. Soc.* **2022**, *144*, 21800−21807. (b) Wu, W.-Q.; Peng, Q.; Dong, D.-X.; Hou, X.-L.; Wu, Y.-D. A dramatic switch of enantioselectivity in asymmetric Heck reaction by benzylic substituents of ligands. *J. Am. Chem. Soc.* **2008**, *130*, 9717−9725. (c) Huang, M.; Wu, Y.-D.; Zhang, X. Mechanistic Insights into Sc(III)-Catalyzed Asymmetric Homologation of Ketones with Diazo Compounds: How Trans Influence Assists in Controlling Stereochemistry. *Chem.—Eur. J.* **2024**, *30*, No. e202303873.

(22) Xiao, B.; Sun, T.-Y.; Zhang, J.; Wu, Y.-D. Theoretical insight into the activity and selectivity in palladium/Ming-Phos-catalyzed three-component asymmetric synthesis of gem-diarylmethine silanes. *Sci. China Chem.* **2023**, *66*, 2817−2827.

(23) Blacquiere, J. M. Structurally-Responsive Ligands for High-Performance Catalysts. *ACS Catal.* **2021**, *11*, 5416−5437.

https://doi.org/10.1021/jacs.5c14810
J. Am. Chem. Soc. 2025, 147, 45210−45220